Science and Technology Indonesia
e-ISSN:2580-4391 *p*-ISSN:2580-4405
Vol. 9, No. 2, April 2024

Research Paper

Formulation and Evaluation of Gambier (*Uncaria gambir*)-Chitosan Microparticle Intranasal Delivery for Alzheimer's Diseases

Najma Annuria Fithri[1]*, Mardiyanto[1], Fitrya[1], Asfaraeni Rahmah[1], Novilia Megi Annisa[1]

[1]*Pharmacy Department, Universitas Sriwijaya, Indralaya, 30862, Indonesia*
***Corresponding author**: najma.fithri@mipa.unsri.ac.id*

Abstract
Alzheimer's Disease (AD), the most common form of dementia continues to be the deadliest neuro degenerative disease in recent years. Despite significant efforts to mitigate the progression of the disease, there is no known cure and development towards a more effective treatment is still lacking. AD is marked by exceptionally low amount of acetylcholine in the brain, formation of tau protein, and amyloid beta plaque. Current drugs of choice for treating AD, namely donepezil and memantine, are acetylcholinesterase (AChE) inhibitors which focused on delaying the onset of cognitive decline by maintaining acetylcholine concentration. Gambier water extract (GWE) contains high level of polyphenols which act as an antioxidant, exhibit strong correlation with AChE inhibitor. The aim of this research is to formulate and encapsulate GWE inside a microparticle system composed of chitosan and different crosslinkers, STPP (IMGS) and $CaCl_2$ (IMGC), which were then characterized as AChE inhibitor using Ellman's method. Variations of the formula were designed following Box-Behnken experimental design with chitosan and crosslinker concentration, crosslinker type, and stirring speed as variables. Initial activity of GWE, IMGS and IMGC as antioxidant were confirmed with DPPH method, obtaining a strong activity of 88.01, 82.11, and 84.99% DPPH inhibition at 100 ppm respectively. Promisingly, at concentration of 100 ppm GWE demonstrated AChE inhibition of 30.36%. However, this activity reduced after encapsulation into IMGS and IMGC, with 14.63% and 18.65% AChE inhibition, which can be linked to the relatively sustained diffusion of GWE from the polymer matrix. IMGS and IMGC diffusion profile showed release of 23.24% and 21.89% after 6 hours, with significant increase in diffusion after 24 hours with 74.92% and 71.19% respectively. Despite showing sustained release behaviour, both IMGS and IMGC ex-vivo diffusion significantly improved when compared to GWE which only diffused 51.84% after 24 hours. This result indicates encapsulation of GWE into a polymeric carrier could increase gambier diffusion through the nasal mucous membrane, significantly improving the potential to penetrate into the brain systemic circulation. Combined with desirable intranasal delivery characteristics, this research was able to demonstrate the promising potential of gambier water extract polymeric system as AChE inhibitors for AD therapy.

Keywords
Intranasal Delivery, Polymeric Encapsulation, *Uncaria gambir*, Alzheimer's Disease, Acetylcholinesterase Inhibitor

Received: 18 December 2023, Accepted: 21 February 2024
https://doi.org/10.26554/sti.2024.9.2.284-298

1. INTRODUCTION

Alzheimer's Disease (AD) is a neurodegenerative disorder characterised by a decrease in cognitive function, orientation, calculation, learning capacity, language, and decision making (Peng et al., 2023; van der Flier et al., 2023). In a 2023 report, AD caused more deaths than breast cancer and prostate cancer combined with poor prognosis. Studies indicate that 1 in 3 people with dementia including AD only have four to eight years of survival post diagnosis (Association, 2023). One of the widely known causes of AD is due to the decrease of acetylcholine concentration impacted by cholinergic nerve degeneration (Arvanitakis et al., 2019; Colovic et al., 2013). Pervin et al. (2014) stated that one of the treatment of Alzheimer is to prevent the decrease of acetylcholine concentration by inhibiting AChE which can be done by giving natural antioxidant that can ward off free radical, which in this research was conducted by utilising antioxidant rich gambier extract.

Indonesia is the world's leading gambier (*Uncaria gambir* Roxb.) exporter with data in 2013 showing 80% of exports originated from Indonesia (Yeni et al., 2014). Among native indigenous population of Malay peninsula and Sumatera, gambier is used as raw material for abdominal pain and toothache (Nazir, 2000). Gambier contains functional compounds belonging to the class of polyphenols, especially catechins. The main components of gambier include catechu tannic acids (20 – 50%), catechins (7 – 33%), and pyrocatechol (20 – 30%). Cat-

echins as the most abundant phytochemical in gambier have activity as antioxidant, antibacterial, antiatherosclerosis and antidiabetic (Anggraini et al., 2011; Kassim et al., 2011; Melia et al., 2015; Pambayun et al., 2007; Yunarto and Aini, 2015). Several studies have shown that the ability to inhibit free radicals from gambir extract is 82.23% (at 50 ppm concentration) with an IC_{50} value of 6.4 ± 0.8 ppm (Kassim et al., 2011; Sazwi et al., 2013). Research shows that the antioxidant activity of ethyl acetate and ethanol extracts is stronger than water extract. However, the properties of ethyl acetate and ethanol that may irritate the nasal mucosa and respiratory tract are taken into consideration when designing intranasal delivery (Apea-Bah et al., 2009; Centers for Desease Control and Prevention, 1978; Departement of Health, 2016).

The intranasal route is one of the potential treatment routes which has been considered in assisting drug delivery to achieve therapeutic benefits for the relatively difficult to penetrate blood brain barrier (BBB) and the central nervous system (CNS) including medication for AD (Taléns-Visconti et al., 2023; Wu et al., 2023a). BBB is typically only permeable towards lipophilic molecules with molecular weight of less than 600 Da and the partition coefficient of 1.5 – 2.7. In addition, BBB is also supplemented by a high number of drug transporters such as polyglycoproteins (PGP) that often inhibit the entry of drugs into CNS (van Woensel et al., 2013). It is these factors that caused BBB as a major barrier for drugs targeting the brain. The difficulty of drug molecules in penetrating the blood brain barrier (BBB) to enter into CNS can be overcome with intranasal delivery, due to the ability of micro and nanosized particles to permeate through the olfactory region (Boyuklieva and Pilicheva, 2022; Wu et al., 2023b). The delivery mechanism and physicochemical properties of drug molecules are the main factors to be considered in designing drug delivery systems targeting the brain. Drug absorption in the olfactory region becomes an option for drugs targeting the brain because of its large absorbing surface area and is the nasal and brain connecting compartment (Boyuklieva and Pilicheva, 2022; van Woensel et al., 2013; Wu et al., 2023a). The nasal mucosa becomes one of the targeted areas in neurotherapy because the mechanism of drug absorption occurs in the nasal mucosa (Kalkotwar et al., 2012; Lee and Minko, 2021; Pardeshi and Belgamwar, 2013).

One way to increase the efficacy of phytocompounds given intranasally is by absorbing or encapsulating the compound with polymers. Chitosan is a saccharide polymer that is commonly utilised in assisting development of intranasal preparations due to advantages including strong mucoadhesive profile, good water solubility, biocompatibility, biodegradability, and economic feasibility (Sachdeva et al., 2023). However, the most important consideration in incorporating chitosan for intranasal delivery is their modality to reversibly open tight junctions by redistribution of proteins, including occludin, ZO-1 and actin-cytoskeletons (Casettari and Illum, 2014; Deli, 2009). To produce chitosan nano or microparticles crosslinking agents were employed by adding sodium tripolyphosphate (STPP) or calcium chloride ($CaCl_2$) (Casettari and Illum, 2014; Sachdeva et al., 2023). STPP is an anionic cross linker that has a positive surface charge suitable for mucosal adhesion application, while $CaCl_2$ is an ionotropic cross linker that can strengthen the chitosan/alginate matrix (Ribeiro et al., 2020). Mechanism of chitosan in modulating tight junction to facilitate permeation of GWE microparticles through the olfactory region can be observed in Figure 1.

This research was conducted by creating and optimizing microparticles of chitosan and crosslinker as carrier of gambier water extract (GWE). Effect of chitosan concentration, cross linking type and concentration as well as stirring speed using were observed using Box-Behnken experimental design to optimise the response produced. Optimum formula from each crosslinking agent (IMGC and IMGS) obtained based on microparticle characteristics were then further analysed for particle size and morphology, intranasal characterisation, diffusion rate and AChE inhibitor activity. By modifying gambier extract into microparticles for intranasal delivery we aim to successfully increase gambier ability to diffuse through biological membrane while maintaining its therapeutic effect, specifically for AChE inhibitor as an alternative therapy for AD.

2. EXPERIMENTAL SECTION

2.1 Materials

Materials used in this research including solvents were pro analysis and pharmaceutical grade. Fresh gambier leaves were obtained at Babat Toman Village, Musi Banyuasin, Indonesia. Acetylcholinesterase (AChE) from *Electrophus electricus*, 5.5'-dithio-bis-2-nitrobenzoic acid (DTNB), acetylcholine iodide, 1,1-diphenyl-2-picrylhydrazyl (DPPH), catechin, gallic acid, and quercetin were all obtained from Sigma-Aldrich, Singapore. Additionally, materials for IMGS and IMGC formulation including chitosan, STPP and CaCl2 were purchased from PT Bratachem Indonesia.

2.2 Methods

2.2.1 Gambier Water Extract Preparation

Fresh gambier leaves were boiled in distilled water for 1.5 hours followed by pressing the boiled leaves to maximise yield of extract. The extract generated was stored in a closed container and then precipitated for 24 hours in room temperature. The resulting precipitate was sun dried in paraku, a wooden molding container (measuring 10 cm × 10 cm × 3 cm) for 24 hours. The extract was then formed and dried with the help of sunlight for three days (Anggraini et al., 2011). Extract was then characterized to determine for quality

2.2.2 Determination of Catechin Content

Preparation of standard catechin solution was conducted by dissolving catechin in ethyl acetate. The resulting solution was then measured by UV-Visible spectrophotometer (Shimadzu® UV-1700) at wavelength of 279 nm. Levels of catechins in the extract can be calculated using linear regression, with extract

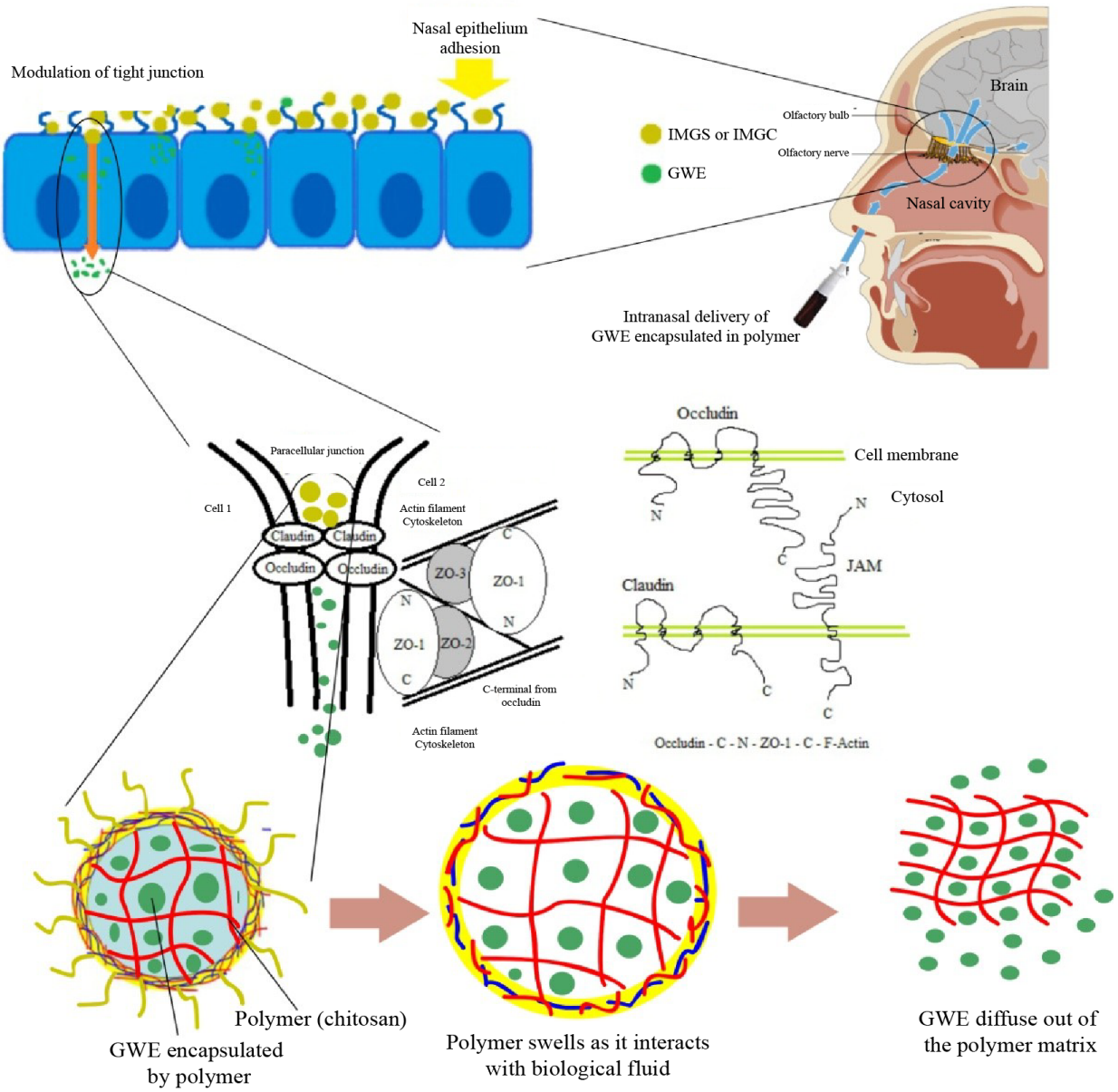

Figure 1. Mechanism of Gambier Extract Delivery into the Brain through the Olfactory Region Assisted by Polymer (Chitosan) as Tight Junction Modulator

concentration (in ppm) as x axis and absorbance value as y ordinate

2.2.3 Determination of Total Phenolic Content

GWE was dissolved with methanol:water (1:1) and then added with 3.95 mL distilled water and 0.25 mL Folin-Ciocalteau reagent. The resulting mixture was then vortexed (Corning® LSE) and incubated in room temperature for 8 minutes. An additional 0.75 mL Na_2CO_3 20% was added, vortexed and incubated for an additional 30 minutes at 37 °C. The absorbance was measured by UV-Vis spectrophotometer at 766 nm characterized by the formation of a blue complex. Determination of phenol content is calculated by Equation 1, with Cekv as equivalent gallic acid content, G as mass of sample, V as volume and fp as dilution of sample.

$$\%\text{Total Phenolic}\,(c) = \frac{Cekv}{G} \times V \times fp \qquad (1)$$

2.2.4 Determination of Total Flavonoid Content

Extract of 5 mg was dissolved into a flask with methanol p.a. One point five mL of GWE was pipetted into a different flask and added 0.1 mL of $AlCl_3$ 10%, 0.1 mL of 1 M sodium acetate and diluted with distilled water. Vortex the solution until ho-

mogeneous and incubate for 30 minutes at room temperature. Measure the absorbance of the extract using a UV-Vis spectrophotometer at maximum wavelength (Fattahi et al., 2014). Determination of flavonoid levels was calculated by Equation 2.

$$\%\text{Total Flavonoid}\,(c) = \frac{Cekv}{G} \times V \times fp \qquad (2)$$

2.2.5 Antioxidant Activity Test of Samples Using DPPH

DPPH 0.3 mM solution was prepared by dissolving DPPH in methanol p.a., then shaken until homogeneous. A total of 1 mL of 0.3 mM DPPH solution was added in 2.5 mL of methanol p.a., vortexed homogeneously in a test tube and allowed to stand for 30 minutes in the dark room. The solution was determined using UV-Vis spectrophotometer at 517 nm. As control quercetin and donepezil were observed compared with GWE, IMGS and IMGC samples. The antioxidant activity test of controls were made in concentrations of 2; 4; 6; 8; and 10 g/mL, while GWE, IMGS and IMGC were in a concentration variation of 20; 40; 60; 80; and 100 g/mL. One mL of DPPH solution 0.3 mM was taken and added with 2.5 mL of the sample from each concentration, vortexed and allowed for 30 minutes in the dark room. The observed color changes and absorption were measured using a UV-Vis spectrophotometer with maximum DPPH wavelength measured at 517 nm (Fithri et al., 2019). Antioxidant activity of the samples was then determined by the amount of DPPH radical uptake resistance by calculating the percentage of DPPH inhibition activity (Equation 3).

$$\%\text{I} = \frac{\text{Control abs} - \text{Sampel abs}}{\text{Control abs}} \times 100\% \qquad (3)$$

2.2.6 Acetylcholinesterase Enzyme (AChE) Inhibition Assay

GWE activity test on AChE was conducted using the colorimetric method of Ellman utilizing acetylcholine iodide (ATCI) as the substrate (Ranjan and Kumari, 2016; Ünver et al., 2016;). The production level of thiocoline was determined by the continuous reaction of thiols with 5.5'-dithiobis-2-nitrobenzoic acid (DTNB) ions to produce a yellow anion of 5-thio-2-nitrobenzoic acid. Briefly in 96-well plates, 25 μL of 15 mM ATCI, 75 l 3 mM DTNB and 50 μL of 50 mM Tris-HCl buffer pH 7.5, containing 0.1% bovine serum albumin (BSA), and 25 l of the samples were added and the absorbance was measured at 405 nm with ELISA reader (Tecan®) after incubation at room temperature for 5 minutes. Donepezil 10% was used as positive control, 10% methanol p.a. in buffer as negative control (enzyme activity without extract), and 50 μL of tris HCl 50 mM pH 7.5 plus 0.1% BSA.The reaction kinetics can be seen within 3 5 minutes. Percentage of enzyme inhibition (% I) of the enzymatic reaction occurring can be calculated using Equation 3.

2.2.7 IMGS and IMGC Intranasal Microparticles Formulation

The optimum formula of microparticle preparation of gambir extract-chitosan was obtained through the experimental design of Box-Behnken. Based on a preliminary test, two crosslinkers were selected STPP and $CaCl_2$. Chitosan polymer and crosslinkers were formulated with GWE concentration of 100 ppm and tween 80 as stabilizers with a concentration of 0.5%. Variations of the formula used to obtain optimum formula can be seen in Tables 1 and 2.

Table 1. Factor and Level Observed in Formulation of GWE Microparticle

Factor	Lower Level	Upper Level
Chitosan concentration (%)	0.1	1
Crosslinking agent concentration (%)	0.1	0.5
Stirring speed (rpm)	400	1500
Crosslinking agent type	STPP	$CaCl_2$

Preparation of microparticles were carried out using ionotropic gelation (Gulati et al., 2013). Chitosan was dissolved in 1% acetic acid and prepared according to the formula shown in Table 2. The solution was then added with GWE and stirred using a magnetic stirrer at room temperature. Addition of tween 80 to the solution was done while stirring constantly until a stable solution is obtained. The STPP and $CaCl_2$ solution was prepared according to the formula and added to the chitosan-extract complex dropwise using a syringe while stirring using a magnetic stirrer at a conditioned speed described in Table 2. Stirring was continued for 30 minutes then the microparticles suspension was centrifuged for 30 minutes at a speed of 6000 rpm (Hettich® Universal 320R).

2.2.8 IMGS and IMGC Evaluation

2.2.8.1 Organoleptic

The intranasal preparations of the resulting microparticles observed for sediment and redispersion ability. Assessment of organoleptic preparation was done by determining its value from 1 - 5 with the following provisions: (1) clump and cohesive deposits such as caking; (2) small clumps of precipitate or agglomerate; (3) settling and difficult to disperse; (4) precipitate but easily dispersed; and (5) not settling.

2.2.8.2 Entrapment Efficiency

Determination of entrapment efficiency was performed using centrifugation and spectrophotometric technique (Gulati et al., 2013). Prior to entrapment efficiency determination, standard curve was determined using catechin as compound of interest. From each formula 10 mL was centrifuged at 6000 rpm for 30 minutes at 20 °C. The resulting supernatant determined at maximum wavelength for absorbance, which then will be calculated for for entrapment efficiency using Equation 4 (Salatin

Table 2. Intranasal Gambier Extract Microparticle Formulation Based on Box-Behnken Design with 3 Variables

Formula	Chitosan Concentration (%)	Crosslinker Concentration (%)	Crosslinker Type	Stirring Speed (rpm)
1	0.55	0.1	STPP	400
2	0.1	0.5	$CaCl_2$	950
3	0.55	0.5	STPP	400
4	0.55	0.3	$CaCl_2$	950
5	0.1	0.1	STPP	950
6	0.55	0.1	$CaCl_2$	400
7	0.55	0.5	$CaCl_2$	400
8	0.55	0.5	$CaCl_2$	1500
9	0.55	0.3	STPP	950
10	0.55	0.1	STPP	1500
11	1	0.5	$CaCl_2$	950
12	0.55	0.3	STPP	950
13	0.55	0.3	$CaCl_2$	950
14	1	0.3	$CaCl_2$	1500
15	0.1	0.1	$CaCl_2$	950
16	0.1	0.3	STPP	400
17	0.55	0.3	$CaCl_2$	950
18	0.1	0.3	$CaCl_2$	400
19	0.1	0.5	STPP	950
20	0.1	0.3	STPP	1500
21	1	0.1	$CaCl_2$	950
22	0.1	0.3	$CaCl_2$	1500
23	0.55	0.3	STPP	950
24	1	0.5	STPP	950
25	0.55	0.1	$CaCl_2$	1500
26	1	0.3	STPP	1500
27	0.1	0.1	STPP	950
28	0.55	0.5	STPP	1500
29	0.55	0.3	STPP	950
30	1	0.3	$CaCl_2$	400
31	0.55	0.3	$CaCl_2$	950
32	1	0.3	STPP	400
33	0.55	0.3	$CaCl_2$	950
34	0.55	0.3	STPP	950

et al., 2017).

$$\%EE = \frac{\text{added drug content} - \text{drug content in supernatant}}{\text{added drug content}} \times 100\% \quad (4)$$

2.2.8.3 Thermodynamic Stability Test

The stability was tested through heating cooling cycle method (Estanqueiro et al., 2014). The test was conducted by storing the microparticles in the refrigerator (4 °C) and oven (40 °C) alternately every 24 hours for 7 days. After the test, the presence or absence of discoloration and precipitate formed as well as the amount of active substance in the preparation was measured following previously described procedure in determination of entrapment efficiency.

2.2.8.4 Sedimentation Time and Volume Test

Two mL from each preparation was inserted into the test tube and set aside at room temperature. The time for the particle dispersion to settle perfectly was recorded. The resulting precipitate was measured in volume and calculated for sedimentation volume.

2.2.8.5 Redispersibility Test

The preparation was stored inside a vial which was then rotated 180° and reversed to its original position. Assessment is performed on the basis of the number of cycles required to completely redisperse the microparticle suspension (Gebresamuel and Gebre-Mariam, 2013).

2.2.8.6 Particle Size and Morphology Characterisation

Determination of particle size, zeta potential, and PDI was performed using particle size Analyser (PSA, Horiba Scientific SZ-100). For morphology analysis transmission electron microscopy (TEM, JOEL JEM 1010) was employed. The optimum formula preparation of 50 μL was diluted with distilled water up to 100 times. A drop of 50 μL dilution was then dropped onto the TEM-grid. The sample was analyzed under focusing digital microscopy with a voltage of 80 kV.

2.2.8.7 FTIR Analysis of GWE, IMGS, and IMGC

The interaction between gambier, chitosan, and other materials can be determined using fourier transform infrared spectrophotometer (FTIR, Shimadzu®). Analysis was performed on GWE, IMGS, IMGC as well microparticles without extract which have been freeze dried (Martin Christ®). The sample preparation was performed by crushing 1 mg of freeze drying nanoparticles with 50 mg of potassium bromide (KBr) and mechanically pressed for the resulting strips. Samples were scanned at wavelength 4000 – 400 cm^{-1}.

2.2.8.8 Pump Delivery

Optimum formulas were sprayed into pre-weighed watch glass and was reweighed to observe the mass released. This process was repeated ten times, and the average weight of the spray produced per spray (individual weights) was calculated. The difference between the weights generated in each experiment should not exceed 6% and should not exceed 10% of the average weight of ten trials (Pawar and Chaudhary, 2015).

2.2.8.9 Spray Weight Uniformity

Priorly weighed intranasal solution were inserted into a specific atomizer for intranasal delivery. Container was shaken for 5 seconds and spray was discarded once to clean the impurities. Then wait for 5 seconds, shaken again for 5 seconds and discard again, repeat this procedure 3 times. The weight at each spray in the solution is collectively determined by evaluating the uniformity of weight in a particular spray. Weighing were done at 6th, 7th, 8th, 82th, 164th, 165th, and 166th spray (Pawar and Chaudhary, 2015).

2.2.8.10 Spray and Geometric Pattern

Pray pattern was tested by spraying the dosage on a plastic sheet of a certain size with a distance of 5 cm. Spray pattern testing was performed three times with observation made on spray pattern formed and its diameter. The spray pattern formed was measured for diameter of the spray produced (Guo and Doub, 2006).

2.2.8.11 Catechin Content Identification

The identification of catechin content of the preparation was done by thin layer chromatography (TLC) method. Stationary phase was silica TLC plate of GF_254 which was inserted into a chamber containing eluent ethyl acetate and methanol mixture with a ratio of 1:1. The Rf value was calculated and compared to the standard catechin Rf value.

2.2.8.12 Ex Vivo Drug Release Assay

Ex vivo drug release was observed using Franz diffusion cell with goat nasal mucous membrane, and phosphate buffer solution pH 6.4 as medium to simulate nasal fluid. The goat nasal membrane was washed with phosphate buffer solution of pH 6.4. Thereafter the membrane was attached to the acceptor and donor connector portion with the membrane dermal portion of the phosphate buffer solution pH 6.4 to the acceptor portion. Tests were performed for three replicates and the test temperature was maintained at 37 ± 0.5 °C with a stirring speed of 100 rpm. Two mL of the optimum formula and GWE samples were placed on the goat nose mucous membrane with a diameter of 18.56 ± 0.44 mm and a thickness of 0.23 ± 0.01 mm (on the donor portion). Sampling was done by taking 2 mL of sample solution on the acceptor part (receptor compartment) at minute 0; 5; 10; 15; 30; 45; 60; 90; 120; 180; 240; 300; 360; and the 24th hour. The solution was replaced with a phosphate buffer solution of pH 6.4 of 2 mL after each sampling to maintain sink condition. The resulting sample was analyzed using a UV-Vis spectrophotometer at catechin predetermined wavelength determined the amount of drug undergoing permeation at any given time interval (Fithri et al., 2017; Fitrya et al., 2021).

3. RESULTS AND DISCUSSION

Based on the results from extract characterisation of GWE, the extract obtained was in accordance with the criteria specified in Indonesian Standard for Extract and Indonesian Herbal Pharmacopoeia (Department Kesehatan Republik Indonesia., 1995; Departemen Kesehatan Republik Indonesia, 2000). Total catechin, flavonoid and phenolic obtained from GWE were 68.15 mg/g extract, 263.30 mgQE/g extract and 312.80 mgGAE/g extract respectively. These results showed GWE contained high number of polyphenols which are needed to exhibit strong antioxidant activity. This result was comparatively higher compared to previous research (Anggraini et al., 2011). The formulation into microparticles (IMGS and IMGC) were able to maintain and preserve gambier polyphenols content shown in Figure 2a. The values obtained were smaller which could be explained by the interference of polymer and crosslinker during the assay. Aside from that the encapsulation process prevent free GWE to interact with the reagents for the assays. Additionally, we also confirmed the presence of catechin based on the TLC result (Figure 2b), which clearly showed catechin after formulation into IMGS and IMGC.

To obtain antioxidant activity, DPPH inhibition assay was conducted to calculate the IC_{50} of GWE, IMGS, IMGC and controls, donepezil HCl and quercetin. DPPH compounds are stable free radical compounds and have the ability to receive hydrogen atoms donated by antioxidants. The existence of this reaction can be observed from the colour change of violet to yellow to clear (Molyneux, 2004). Antioxidant activity was assessed from the ability of sample to inhibit DPPH by calculating absorbance value (Baliyan et al., 2022). IC_{50} of

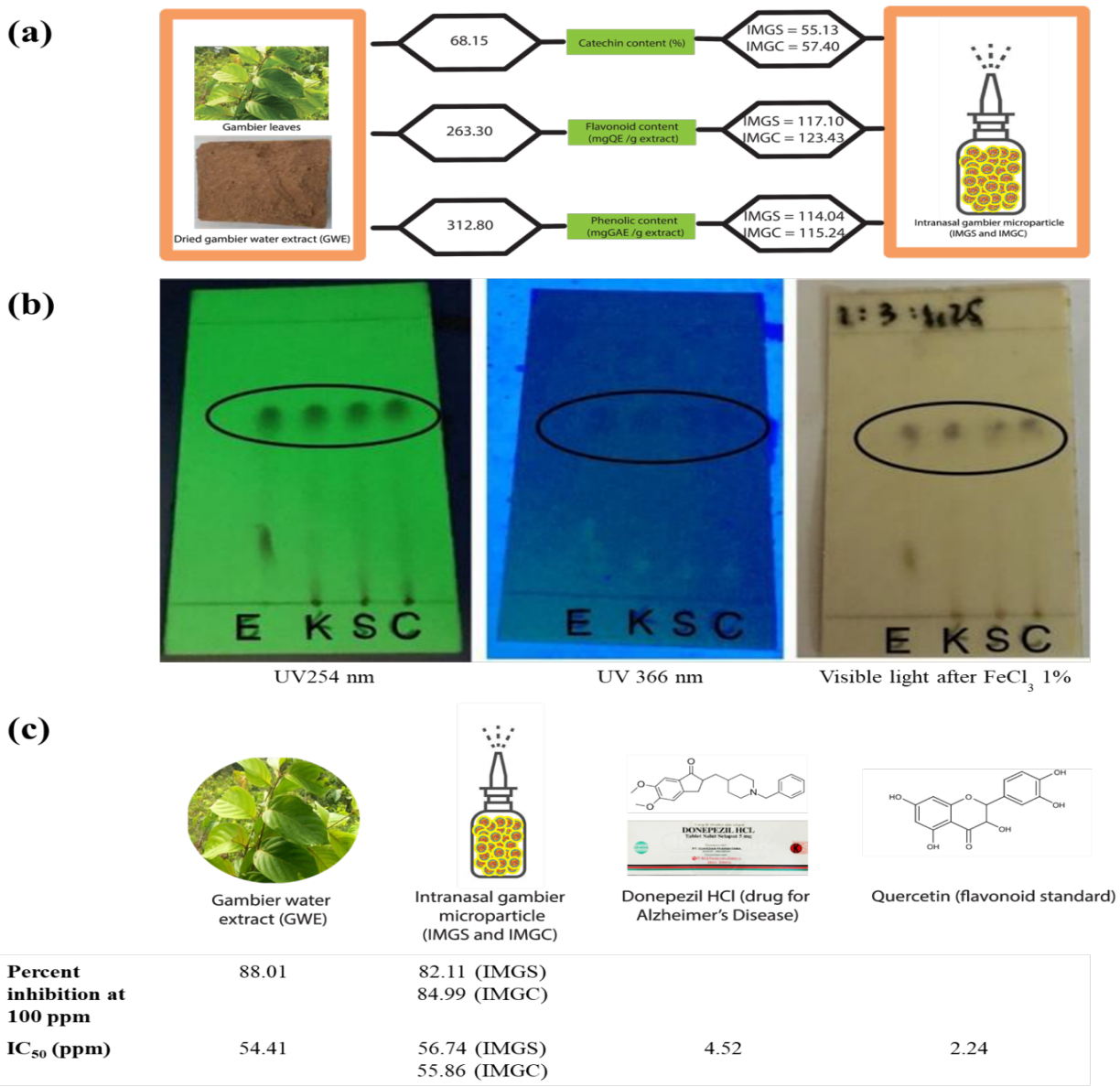

Percent inhibition at 100 ppm	88.01	82.11 (IMGS) 84.99 (IMGC)		
IC_{50} (ppm)	54.41	56.74 (IMGS) 55.86 (IMGC)	4.52	2.24

Figure 2. Results Obtained from Various Assays, Including Catechin, Flavonoid and Phenolic Content in Free Non-Formulated GWE and Formulated IMGS/IMGC (a). TLC Observation of Catechin Presence Under UV and Visible Light in GWE (E, catechin standard (K), IMGS (S), and IMGC (C) (b). Antioxidant Activity of GWE, IMGS and IMGC Compared to Positive Control Donepezil HCl and Quercetin (c).

GWE, IMGS and IMGC that were obtained are 54.41, 56.74 and 55.86 ppm respectively, which is considered a strong antioxidant (Molyneux, 2004). Although when compared to the controls (Figure 2c), both donepezil HCl and quercetin exhibited stronger antioxidant effect, due to the purity of GWE being less than pure compounds such as quercetin and active pharmaceutical ingredient. It also worth noting the antioxidant activity of GWE and its subsequent intranasal formulations were stronger than many Indonesian herbal extracts including from *Curcuma xanthorriza* and *Phyllantus niruri* (Sukweenadhi et al., 2020).

After determining the strong antioxidant effect of GWE, formulation of intranasal microparticle containing GWE was optimized based on Box-Behnken design. Variables observed in this research were considered to have significant effect towards the characteristics of the resulting microparticle formulation, namely concentration of chitosan and crosslinker, crosslinker type and stirring speed. To obtain optimum formula, analysis was conducted based on the tests results from the 34 formulas of Box Behnken design shown in Table 3.

Organoleptic observation of intranasal preparations on the first day relates to the size of the particles produced during the

Table 3. Results of 34 Box-Behnken Formula of Gambier Intranasal Microparticle

Formula	Organoleptic Day 1	Organoleptic Day 45	Encapsulation Efficiency (%)	pH	Stability Content (ppm)	Sedimentation Time (s)	Redispersibility	Sedimentation Volume
1	4	3	92.99 ± 0.02	6.85	64.62 ± 0.75	32 ± 1.00	3.33 ± 0.58	0.39
2	5	3	91.22 ± 0.02	4.43	75.77 ± 0.05	120.67 ± 1.53	2.67 ± 0.58	0.03
3	4	3	90.74 ± 0.04	7.3	74.84 ± 0.68	86.67 ± 3.06	2.33 ± 0.58	0.24
4	4	4	93.72 ± 0.05	5.86	69.87 ± 0.26	101.67 ± 2.52	1 ± 0	0.11
5	4	3	79.31 ± 0.06	6.63	64.35 ± 0.27	37.67 ± 1.53	1.33 ± 0.58	0.18
6	4	2	89.73 ± 0.05	5.97	59.56 ± 0.05	52.33 ± 1.53	2 ± 0	0.17
7	4	4	97.44 ± 0.05	6	82.84 ± 0.19	44.33 ± 2.08	1.33 ± 0.58	0.06
8	5	3	93.21 ± 0.06	5.66	55.26 ± 0.02	58 ± 1.00	2.33 ± 0.58	0.08
9	2	2	92.85 ± 0.08	7.33	51.81 ± 0.24	51.67 ± 1.53	7.33 ± 0.58	0.19
10	4	4	95.03 ± 0.04	6.12	55.85 ± 1.32	103.33 ± 3.51	1.67 ± 0.58	0.20
11	4	3	92.24 ± 0.05	6.01	64.21 ± 0.38	56.33 ± 1.16	2.33 ± 0.58	0.08
12	2	2	91.82 ± 0.05	7.37	50.24 ± 1.01	57.67 ± 1.53	7.67 ± 0.58	0.18
13	4	3	93.33 ± 0.11	5.64	68.37 ± 1.01	64.67 ± 2.08	1 ± 0	0.08
14	4	3	91.79 ± 0.84	6.06	77.79 ± 0.53	89.67 ± 2.08	2.67 ± 0.58	0.12
15	5	3	89.33 ± 0.12	4.77	53.61 ± 0.09	56.33 ± 1.53	1 ± 0	0.03
16	4	4	91.34 ± 0.06	6.69	53.12 ± 0.75	336.67 ± 13.32	1 ± 0	0.17
17	4	3	94.42 ± 0.56	5.62	66.94 ± 0.45	56.33 ± 0.58	1 ± 0	0.14
18	5	3	90.68 ± 0.18	4.61	60.90 ± 0.29	61.33 ± 2.08	2 ± 0	0.03
19	4	4	80.22 ± 0.02	7.32	51.01 ± 0.15	91.67 ± 2.08	2 ± 0	0.37
20	4	4	84.35 ± 0.09	6.5	56.04 ± 0.04	387 ± 9.85	1.67 ± 0.58	0.17
21	4	4	96.28 ± 0.25	5.9	79.98 ± 0.09	490.67 ± 11.93	1.33 ± 0.56	0.17
22	4	3	81.77 ± 0.04	4.58	65.90 ± 0.03	37.67 ± 1.16	1 ± 0	0.02
23	2	2	94.04 ± 0.22	7.3	63.74 ± 0.16	133 ± 3.61	7.67 ± 0.5774	0.17
24	4	4	92.39 ± 0.08	7.62	60.56 ± 0.19	123.33 ± 2.52	4.33 ± 0.5774	0.14
25	4	3	91.71 ± 0.07	5.58	66.59 ± 0.57	214.67 ± 4.04	1.67 ± 0.5774	0.13
26	3	3	90.05 ± 0.08	7.49	54.46 ± 0.09	308.33 ± 6.81	2.67 ± 0.5774	0.17
27	4	4	93.95 ± 0.05	5.08	62.39 ± 0.11	758.67 ± 34.93	1 ± 0	0.17
28	4	3	88.04 ± 0.09	7.45	51.27pm0.12	59 ± 2	1.33 ± 0.5774	0.11
29	2	2	79.59 ± 0.14	7.24	63.54 ± 0.19	60.33 ± 2.08	7 ± 1	0.15
30	4	2	89.97 ± 0.07	5.89	70.83 ± 0.21	618 ± 10	1 ± 0	0.08
31	4	2	95.64 ± 0.06	5.53	68.42 ± 0.70	350.67 ± 7.51	1 ± 0	0.06
32	4	2	92.09 ± 0.05	7.36	83.73 ± 0.21	84.333 ± 1.53	2.33 ± 0.5774	0.08
33	4	3	98.67 ± 0.10	5.52	74.92 ± 0.19	226.33 ± 11.01	1.33 ± 0.5774	0.05
34	1	1	93.40 ± 0.16	7.24	72.79 ± 0	146.33 ± 2.08	11.67 ± 0.56	0.14

manufacturing process. Chitosan concentrations affects the size of microparticles leading to the possibility of aggregation which can trigger the process of sedimentation and instability to the formulation (Rajaram and Natham, 2013). Particle size particularly also impacted redispersibility, as sedimentation tends to increase molecular interaction hindering ease of redispersion (Mardiyanto et al., 2019). Redispersibility depends on the particle size in the dispersed phase and the resulting sedimentation form (flocculant, nonflocculant, or coagulant). Particles that produce flocculant form will be more easily dispersed than non-flocculant forms. The type of crosslinker affected the formulation based on the result of interaction or bond obtained through cross linking process. Less crosslinking formed between particles generated larger particles causing segregation of particles so that larger particles settled and over time will form sedimentation (Ribeiro et al., 2020).

According to Gulati et al. the percentage of entrapment efficiency (EE) obtained depends on the type of polymer used and the solubility of the drug in the polymer (Gulati et al., 2013). Chitosan is a hydrophilic polymer which in salt form is produced from reaction with organic acids such as acetic acid. GWE is a water-based extract facilitating ease of absorption into the chitosan matrix. It is noted that increasing concentration of chitosan will increase the EE percent as the viscosity increase causing reducing particle porosity which indirectly yields a more resistant chitosan-extract matrix (Casettari and Illum, 2014; Wu et al., 2023b). An increase in polymer concentration will increase drug uptake. However, too high a polymer concentration can also cause difficulty for GWE to diffuse into the polymer and it can be concluded that chitosan as a polymer has the optimum concentration to absorb the active substance (Caetano et al., 2016; Casettari and Illum, 2014). High stirring speed will result in smaller droplet or particle size caused by the breakdown of chitosan length chains and matrix. Longer chitosan chains have more reactive sides to absorb and bind to extracts so that their EE percent will increase (Rajaram and Natham, 2013).

Another important factor in determining the quality and safety of intranasal preparations is pH. Desirable pH for intranasal preparation is between 4.5 to 6.5, adjusting to nasal mucosal membrane conditions. Acquiring formulation within the desired pH will minimise the occurrence of mucous membrane irritation and to maintain activity of lysozymes responsible for destruction of unwanted bacteria in the nasal cavity

(Al Harthi et al., 2019; Ramvikas et al., 2017). In addition, the pH condition of the nasal mucous membrane and the preparation will affect the percentage of unionized drugs that can be absorbed by the nasal mucous membranes (Kushwaha et al., 2011). Chitosan and crosslinker concentration have significant effect towards final product pH as each of the materials used has a different pH, specifically chitosan which has a more acidic pH due to being dissolved in dilute acetic acid.

Thermodynamic stability tests were performed using stress testing to determine the resistance of the preparations when stored in various temperature. Drugs can undergo various chemical reactions triggered by a change in temperature, which in this formulation can affect the rate of degradation of GWE. Increasing the temperature can increase the reaction rate because of more rapid movement of particles leading to an increase in collision between particles in accordance with Arrhenius theory (Sinko, 2023). The value of this stability is influenced by the particle's ability to prevent flocculation or particle aggregation. A partial micro dispersion system will be stable if it has a strong repulsion energy to prevent flocculation or aggregation. The degree of particles aggregation is influenced by components in a formulation and its physicochemical properties (Akhter and Alam, 2023).

Sedimentation time showed the rate of a dispersion system to form sedimentation, the longer the more stable with relatively uniform size based on the absence of aggregation in dispersion system. While sedimentation volume referred to the volume of sediment produced after a dispersion system is allowed to stand for 48 hours. Noting from our observations, when concentration of chitosan increased, the rate of sedimentation decreased, potentially by the increase in viscosity. As the viscosity increases, the particles will diffuse through the dispersion system, so the time required for the particles to settle is longer (Jonassen et al., 2012). Medium that has a higher viscosity (in this case a high concentration of chitosan solution) produced longer sedimentation rate. Another factor that affected sedimentation time is the particle size of the dispersed phase, which is impacted by stirring speed. The larger particles have a faster sedimentation time because of the greater molecular weight, making it easier to sediment with the force of gravity (Sinko, 2023). Generally, the longer the sedimentation rate will result in a more stable formulation.

With the consideration taken from the tests conducted on the 34 formulas, we analysed the results using Design Expert® 11 (Stat-Ease Inc) and chose two optimum conditions with different crosslinkers. With STPP the optimum condition was 0.1% chitosan, 0.1% STPP and 1200 rpm stirring speed (IMGS), while for $CaCl_2$ optimum condition was 0.16% chitosan, 0.5% $CaCl_2$ and 580 rpm stirring speed (IMGC). These two formulas were then further analysed for particle size, morphology, diffusion profile, FTIR interaction, intranasal characteristics and most importantly AChE inhibitor effect.

Particle size plays an important role in the physicochemical and biological characteristics of particles (Rajaram and Natham, 2013). Measurements of particle size and polydispersity index were performed using PSA where the formulations are diluted with attenuator value ~ 7. This light scattering will be detected and particle size and polydispersity index (PDI) results can be obtained. Result of PSA analysis including z-average value and PDI can be seen in Figure 3a. IMGS formula has a larger particle size possibly due to the lower crosslinker concentration, resulting in a more rigid matrix compared to IMGC. Both PDI values of IMGS and IMGC were greater than 0.5, which can be considered less uniform or polydisperse. In the process of manufacture of the microparticles, there were no sonication or high-speed homogenization involved. For future developments, it is recommended that sonication or homogenization is employed to create smaller and more uniform particles (Mardiyanto et al., 2019).

One of the indices of microparticle stability is determined by its potential zeta value. The theory states that if a particle micro has a larger potential zeta value, then the surface charge of the particle becomes larger, allowing for less interaction of the similarly charged dispersed particle (repulsion effect). Based on studies that have been reported, zeta potential can predict the stability of colloidal micro particles based on barrier energy between particles. As the potential zeta value approaches ± 30 mV, aggregation is increasingly preventable and micro-particle stability increases (Caetano et al., 2016). Zeta potential obtained of IMGC was ±9.5 mV, indicating that the particles produced has lower charge than normally stable particles. The result obtained is positively charged because of the amount of NH_3 ions from chitosan on the surface of the particle.

Particle morphology was analysed using TEM to determine the shape of the resulting particles. The optimum formula IMGC was chosen to be observed based on the PSA analysis. Based on the results obtained on two different magnifications, 500x (left) and 250x (right), the particles obtained were ~ 250 nm in diameter (Figure 3b). TEM image showed smaller particles compared to the z-average due to the polydispersity of the formula obtained. It is recommended to use smaller magnification to obtain higher population of particles or to use more concentrated solution for TEM analysis. The image showed that the resulting particles were spherical with the carrier polymer (chitosan) encasing GWE.

To determine microparticle matrix interaction with gambier extract was performed using FTIR spectrophotometer. The tests were performed on GWE, blank IMGS and IMGC (microparticles blank without extract), IMGS and IMGC microparticles at wavelength 4000 - 400 cm^{-1} (Figure 3d). This test aimed to determine the presence of specific functional group and whether there is any new interaction formed after formulation of GWE into intranasal preparation. Based on the spectra obtained, there is a new peak of the four spectra analyzed when compared with the spectra of GWE. This showed the spectra of chitosan polymer at the wavelength of 2930 – 2920 cm^{-1}. Another difference found in the five spectra was the intensity marked by changes in the transmittable value generated, except between the micro particles $CaCl_2$ with extracts

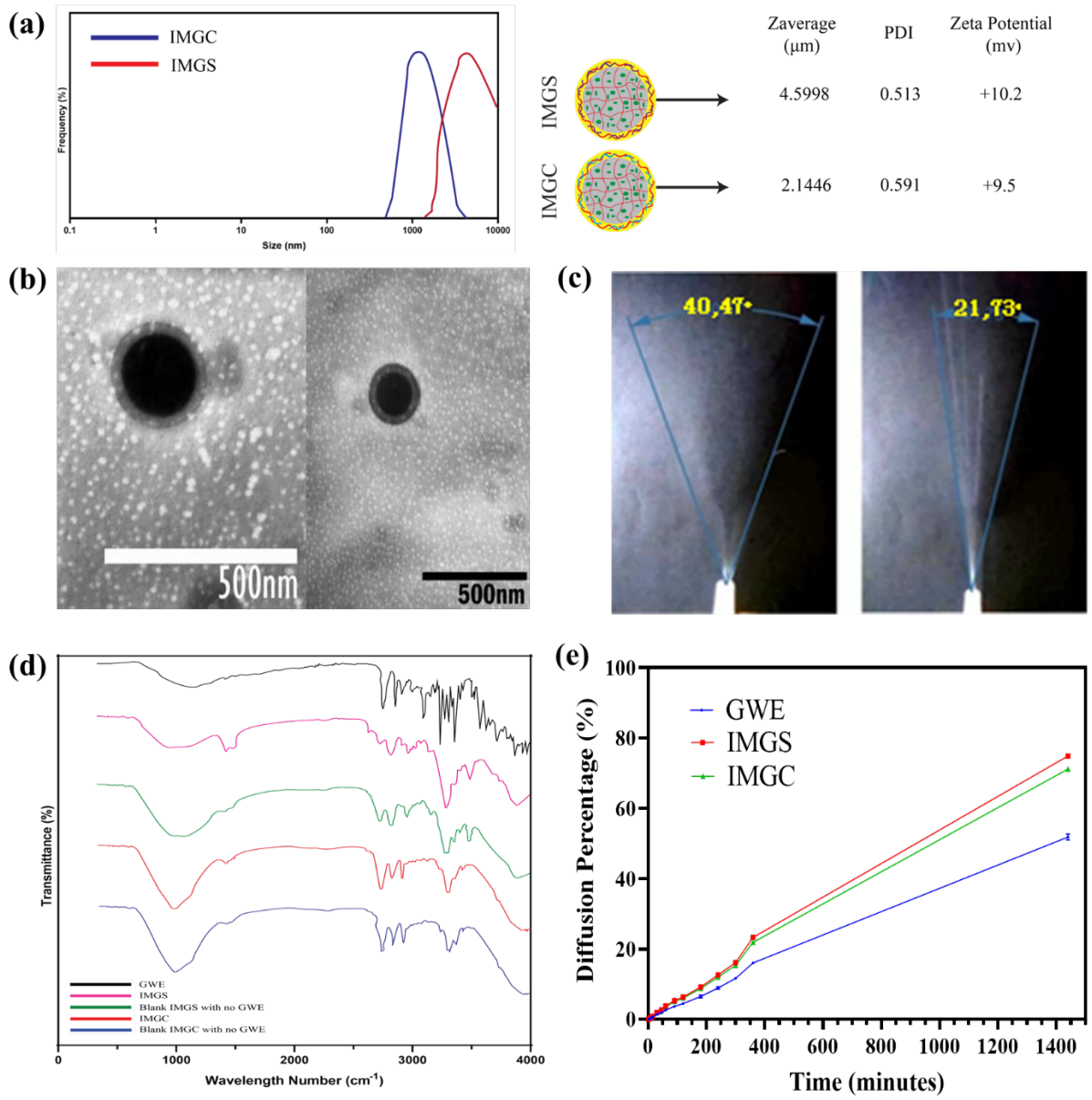

Figure 3. PSA Analysis of IMGS and IMGC Obtaining Particles in Microsized Range with Positive Charge (a). TEM Analysis of the Smaller Sized Formula IMGC, Confirming the Shape of the Microparticle Obtained (b). Spray Pattern and Angle from the Intranasal Atomizer Nozzle (c). FTIR Spectra of GWE and the Formulation with and without the Extract (d). Diffusion Percentage Observed for 1440 Minutes (24 hours), Comparing the Diffusion Profile through Nasal Membrane of GWE, IMGS and IMGC (e).

and blanks that have almost identical spectra. The lower the pH produced after the crosslinker process the lower the % T (Bhumkar and Pokharkar, 2006). The main difference between the extract and the resulting preparations was the appearance of peak at 2922 - 2927 nm. This functional group represents a new functional group appearing in the preparation showing the presence of asymmetric C−H methylene ($-CH_2$). This indicated that IMGS and IMGC have methylene group not present in the extract formed due to the presence of chitosan polymers not present in the extract alone. Chitosan polymer has a methylene group in its structure so it is detected on the IR spectra (Coates, 2000).

Pump delivery test aims to determine the reproducibility of each spray produced in the performance assessment of the drug product and to evaluate the measurement capabilities of the used spray device (Kalkotwar et al., 2012). The ability of the pump delivery will affect the dose delivered at each spray so as to affect the effectiveness of the resulting preparation so that

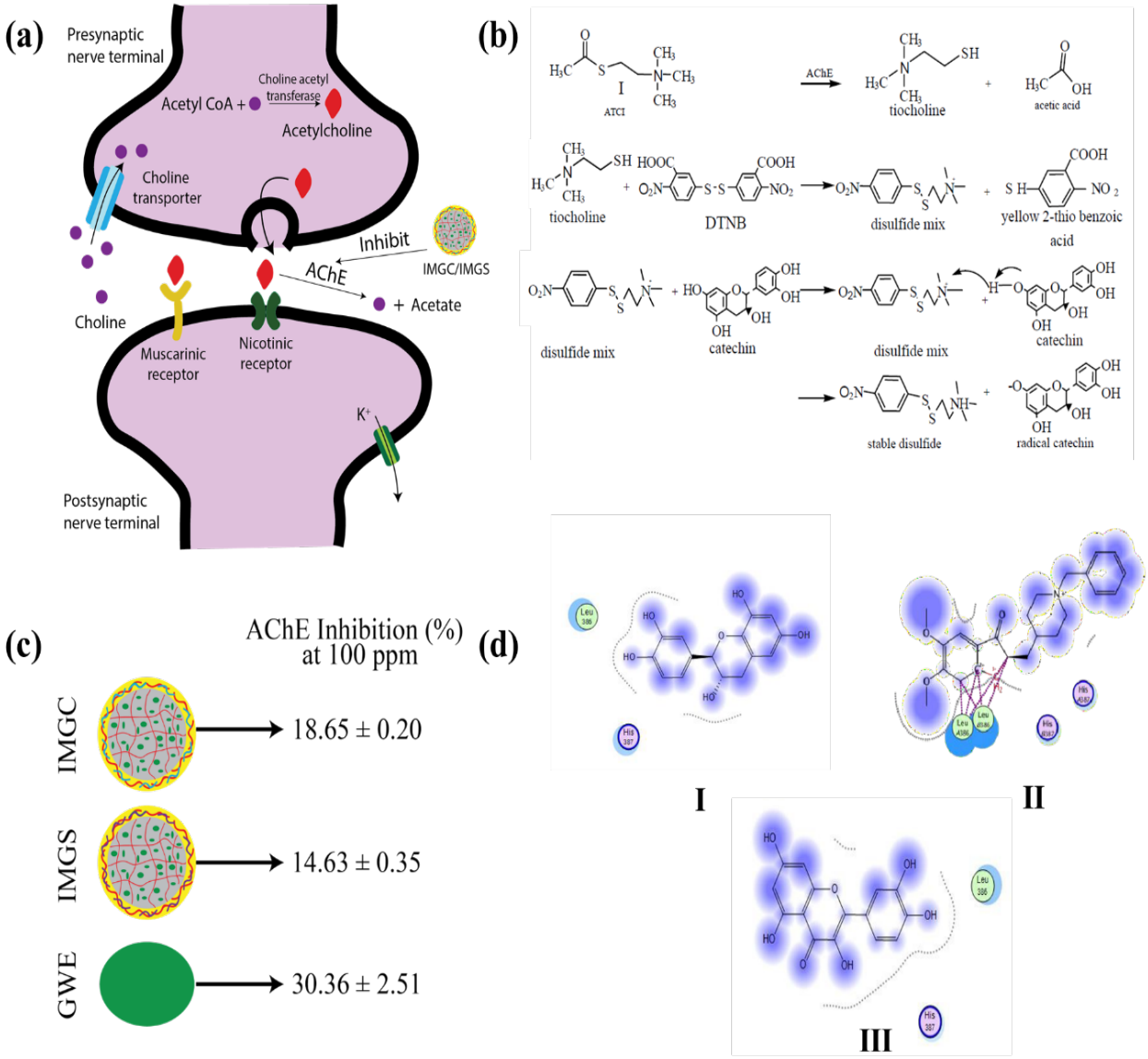

Figure 4. Mechanism of GWE, IMGS or IMGC Impacting Acetylcholine Concentration in the Brain, which is by Inhibiting AChE to Prevent Conversion of Acetylcholine to Choline (a). Mechanism of AChE Inhibition Analysis Following Ellman's Method Using Actylcholine Iodide (ATCI) and 5,5'-Dithio-bis-2-Nitrobenzoic Acid (DTNB) (b). AChE Inhibition Activity of GWE, IMGS and IMGC at 100 ppm (c). Analysis of Ligand Interaction between Catechin (I), Donepezil (II) and Quercetin (III) with AChE Receptor (d)

the ability of the spray pump should be ensured to maintain the quality of the preparation. Based on the results of IMGS, there are four sprays that do not meet the pump delivery requirements of spraying to 2, 3, 7, and 8. IMGS formula has larger particles that has the tendency to form aggregates, clumping and blocking the actuating pump from exerting the accurate dosage leading to non-uniform pump sprays. However, IMGC demonstrated better pump delivery due to smaller sized microparticles maintaining better homogeneity compared with IMGS so that the spraying results were more uniform.

Spray weight uniformity testing was performed to determine the uniformity of the weight of the dosage delivered by the atomiser nozzle in each actuation. The weight of each actuation delivered should be uniform to maintain the uniformity of the dose delivered by each delivery. The uniformity of weights obtained can determine the performance of the nose piece, formulation, method of manufacture, and efficiency of the pump used. The weights analyzed were the weights in administering a single dose in one actuation (Kalkotwar et al., 2012). Table 4 shows the results of the optimum formula spray

Table 4. IMGS and IMGC Spray Pattern and Viscosity Analysis Results

Sample	Spray Pattern			Viscosity	
	Diameter ± SD (cm)	Note	%CV of Spray Weight	Flow (s)	Viscosity (cPs)
IMGS	4.39 ± 0.32	Spray pattern spread evenly and round	> 5%	2.43	1.93
IMGC	4.56 ± 0.16	Spray pattern spread evenly and round	5%	4.86	3.85

weight uniformity test with crosslinker STPP. The tests were performed on several actuation points at the beginning (spray no. 6, 7, and 8), middle (no.82), and end (no. 164, 165, and 166). This is intended to ensure the uniformity of weight generated from the beginning of spraying to spraying at the end of the remaining volume of the preparation. Based on the results of testing on the optimum formula IMGC, all the weights on each actuation have met the requirements and the coefficient of variation generated < 5% so it can be summarized that spray pattern and weight generated were uniform. However, IMGS coefficient variation was > 5%, indicating that IMGC produced better spray pattern and homogeneity result compared to IMGS to the difference in the resulting dispersion system. IMGS formula produced particle deposits which precipitate and possibly interfere with the projectile of microparticle the atomiser pump.

Geometry and spray pattern is done to know the spread and homogeneity of spray spraying distribution area. This parameter can also determine the performance of nozzle and pump (Kalkotwar et al., 2012). Spray pattern testing is done by spraying the dosage on a plastic sheet covered with millimeter block paper to measure the diameter directly. Spraying was done at a distance of 5 cm which is the optimum spraying distance from the nasal cavity to the olfactory mucosa (Guo and Doub, 2006). Observations were made on the diameter and the resulting spraying form. Based on the diameter of the spray produced from IMGS and IMGC, we observed no significant difference between the two formulas. The resulting pattern of dispersion spreads evenly and is almost rounded or circular. The density produced at each spraying is almost uniform. IMGS spray geometry was slightly wider (40.47°) compared to IMGC (21.73°) which was characterised by greater spray angle (Figure 3c). This result could be due to the viscosity of both formulas, where IMGC has slightly bigger viscosity than IMGS. IMGC has higher chitosan concentration (0.161%) than the IMGS formula (0.1%) causing higher viscosity value (Table 4).

Diffusion profile of GWS, IMGS and IMGC were conducted using Franz diffusion cell performed at 37 ± 0.5 °C, 100 rpm stirring speed and freshly obtained goat nasal cavity was used, aimed to mimic physiological mucosal membrane condition. Diffusion percentage comparison between GWE, IMGS, and IMGC demonstrated improved diffusion from the microparticles formulation compared to pure extract. Permeation of the extract through mucosal membrane occurs due to the opening of the tight junction of the cell membrane facilitated by the ability of chitosan modulating tight junction proteins (Casettari and Illum, 2014; Deli, 2009). After 24 hours of observation, both IMGS and IMGC showed significantly higher diffusion percentage of 74.92 and 71.19% compared to unmodified GWE with 51.84% (Figure 3e).

To confirm the ability of GWE and the intranasal formulation in inhibiting AChE, inhibition assay following Ellman's method was conducted on GWE, IMGS and IMGC. Ellman's method is based on a colorimetric reaction between ATCI (a choline substrate) and DTNB, the colour reagent. If little to none presence of AChE exist in the mixture, reaction between ATCI and DTNB resulted into a yellow product thio-2-nitrobenzoate product (Figure 4b) (Pohanka et al., 2011). In this research we used AChE from *Electrophus electricus* as the enzyme. As can be observed in Figure 4c, all samples including free extract and microparticles produced AChE inhibition at 100 ppm of concentration. Lower AChE inhibition in IMGS and IMGC could be explained by the encapsulation of GWE with chitosan polymer and the sustained diffusion profile of both microparticles. Additionally, in silico observation was compared between catechin (Figure 4d (I)), donepezil (Figure 4d (II)), and quercetin (Figure 4d (III)) using Molecular Operating Environment (MOE). Catechin and quercetin were chosen as to represent the major active phytocompounds in GWE and the formulation, while donepezil is the current drug of choice for AD. As can be seen from the picture, pharmacophore from the three compounds interacted with AChE receptor on Leucine 386 and Histidine 387. Histidine 387 structures tend to have more N atomic components than Leucine which lead them to bind more easily under alkaline conditions. The carbon aliphatic chain from the structure of the amino acid leucine 386 will also tend to encourage this amino acid to have a higher degree of hydrophobicity when compared to histidine which has an aromatic carbon chain with 2 N atoms in the constituent ring. From Figure 4a, it is illustrated how intranasal microparticles containing GWE could lead to the increase of acetylcholine in the brain environment by preventing acetylcholine degradation by AChE.

4. CONCLUSIONS

To conclude, we have demonstrated the ability of encapsulating gambier water extract into a microsized polymeric carrier to improve diffusion and permeability through the mucosal membranes. Formulated intranasal microparticles showed good stability and desirable intranasal characteristics with reproducible spray content. Furthermore, the modified gambier intranasal formula were able to maintain antioxidant and AChE inhibition activity. Although, it is worth noting that decreased antioxidant

and AChE inhibitor activity was observed after modification into microparticles, hence it is recommended for future studies to develop a more robust delivery system that could preserve the strength of gambier extract activity. Overall, this research was able to produce stable microparticles and have shown gambier AChE inhibitor activity for potential alternative therapy in combating Alzheimer's Disease.

5. ACKNOWLEDGMENT

Authors would like to express their gratitude towards Pharmaceutical Science and Phytopharmaceutical Group Sriwijaya University for their contribution in discussion of methodology and Pharmaceutical Technology Laboratory Team for the assistance in data gathering.

REFERENCES

Akhter, M. and M. M. Alam (2023). *Ionization and Ionic Equilibria*. Springer Nature Switzerland, Cham, pages 55–77

Al Harthi, S., S. E. Alavi, M. A. Radwan, M. M. El Khatib, and I. A. AlSarra (2019). Nasal Delivery of Donepezil HCl-Loaded Hydrogels for the Treatment of Alzheimer's Disease. *Scientific Reports*, **9**(1); 9563

Anggraini, T., A. Tai, T. Yoshino, and T. Itani (2011). Antioxidative Activity and Catechin Content of Four Kinds of *Uncaria gambir* Extracts from West Sumatra, Indonesia. *African Journal of Biochemistry Research*, **5**(1); 33–38

Apea-Bah, F., M. Hanafi, R. Dewi, S. Fajriah, A. Darwaman, N. Artanti, P. Lotulung, P. Ngadymang, and B. Minarti (2009). Assessment of the DPPH and α-Glucosidase Inhibitory Potential of Gambier and Qualitative Identification of Major Bioactive Compound. *Journal of Medicinal Plants Research*, **3**(10); 736–757

Arvanitakis, Z., R. C. Shah, and D. A. Bennett (2019). Diagnosis and Management of Dementia. *Jama*, **322**(16); 1589–1599

Association, A. s. (2023). Alzheimer's Disease Facts and Figures. *Alzheimers Dement*, **19**(4); 1598–1695

Baliyan, S., R. Mukherjee, A. Priyadarshini, A. Vibhuti, A. Gupta, R. P. Pandey, and C.-M. Chang (2022). Determination of Antioxidants by DPPH Radical Scavenging Activity and Quantitative Phytochemical Analysis of *Ficus Religiosa*. *Molecules*, **27**(4); 1326

Bhumkar, D. R. and V. B. Pokharkar (2006). Studies on Effect of pH on Cross-Linking of Chitosan with Sodium Tripolyphosphate: A Technical Note. *Aaps Pharmscitech*, **7**(2); 138–143

Boyuklieva, R. and B. Pilicheva (2022). Micro-and Nanosized Carriers for Nose-To-Brain Drug Delivery in Neurodegenerative Disorders. *Biomedicines*, **10**(7); 1706

Caetano, L. A., A. J. Almeida, and L. M. Gonçalves (2016). Effect of Experimental Parameters on Alginate/Chitosan Microparticles for BCG Encapsulation. *Marine Drugs*, **14**(5); 90

Casettari, L. and L. Illum (2014). Chitosan in Nasal Delivery Systems for Therapeutic Drugs. *Journal of Controlled Release*, **190**; 189–200

Centers for Desease Control and Prevention (1978). *Occupational Health Guideline for Ethyl Acetate*. Centers for Desease Control and Prevention, Atlanta, US

Coates, J. (2000). *Interpretation of Infrared Spectra, a Practical Approach*. 10815–10837. Encyclopedia of Analytical Chemistry

Colovic, M. B., D. Z. Krstic, T. D. Lazarevic-Pasti, A. M. Bondzic, and V. M. Vasic (2013). Acetylcholinesterase Inhibitors: Pharmacology and Toxicology. *Current Neuropharmacology*, **11**(3); 315–335

Deli, M. A. (2009). Potential Use of Tight Junction Modulators to Reversibly Open Membranous Barriers and Improve Drug Delivery. *Biochimica et Biophysica Acta (BBA)-Biomembranes*, **1788**(4); 892–910

Departemen Kesehatan Republik Indonesia (2000). *Parameter Standar Umum Ekstrak Tumbuhan Obat*. Departemen Kesehatan Republik Indonesia, Jakarta, Indonesia (In Indonesia)

Departement of Health (2016). *Right to Know Hazardous Substance Fact Sheet*. Departement of Health, New Jersey, USA

Department Kesehatan Republik Indonesia. (1995). *Materia Medika Indonesia Jilid VI*. Department Kesehatan Republik Indonesia., Jakarta, Indonesia (In Indonesia)

Estanqueiro, M., J. Conceição, M. H. Amaral, D. Santos, J. B. Silva, and J. M. S. Lobo (2014). Characterization and Stability Studies of Emulsion Systems Containing Pumice. *Brazilian Journal of Pharmaceutical Sciences*, **50**(2); 361–369

Fattahi, S., E. Zabihi, Z. Abedian, R. Pourbagher, A. M. Ardekani, A. Mostafazadeh, and H. Akhavan-Niaki (2014). Total Phenolic and Flavonoid Contents of Aqueous Extract of Stinging Nettle and in Vitro Antiproliferative Effect on Hela and BT-474 Cell Lines. *International Journal of Molecular and Cellular Medicine*, **3**(2); 102

Fithri, N. A., F. Fitrya, T. Shabrina, and D. Yulanri (2019). Antioxidant Activity Analysis and Standardization of *Parkia Speciosa* (Petai) Pods Ethanol Extract. *Science and Technology Indonesia*, **4**(1); 5–10

Fithri, N. A., M. Mardiyanto, R. P. Novita, and V. Andrean (2017). Furosemide Self Nano Emulsifying Drug Delivery System (SNEDDS) Formulation Comprising of Capryol-90, Polysorbate-80, and Peg-400 with Simplex-Lattice-Design. *Science and Technology Indonesia*, **2**(4); 85–88

Fitrya, F., N. A. Fithri, A. Amriani, A. Haryati, and D. P. Wijaya (2021). Preparation and Characterization of Petai Pods Extract (*Parkia speciosa* Hassk.) Loaded Ethosomes. *Science and Technology Indonesia*, **6**(1); 19–24

Gebresamuel, N. and T. Gebre-Mariam (2013). Evaluation of the Suspending Properties of Two Local Opuntia spp. Mucilages on Paracetamol Suspension. *Pakistan Journal of Pharmaceutical Sciences*, **26**(1); 23–29

Gulati, N., U. Nagaich, and S. A. Saraf (2013). Intranasal Delivery of Chitosan Nanoparticles for Migraine Therapy. *Scientia Pharmaceutica*, **81**(3); 843–854

Guo, C. and W. H. Doub (2006). The Influence of Actuation

Parameters on in Vitro Testing of Nasal Spray Products. *Journal of pharmaceutical sciences*, **95**(9); 2029–2040

Jonassen, H., A.-L. Kjøniksen, and M. Hiorth (2012). Stability of Chitosan Nanoparticles Cross-Linked with Tripolyphosphate. *Biomacromolecules*, **13**(11); 3747–3756

Kalkotwar, R. S., V. V. B. Patil, A. M. Patel, S. D. Tathe, and S. S. Rawat (2012). Evaluation and Quality Control of Nasal Spray. *Journal of Drug Delivery and Therapeutics*, **2**(4); 1–4

Kassim, M. J., M. H. Hussin, A. Achmad, N. H. Dahon, T. K. Suan, and H. S. Hamdan (2011). Determination of Total Phenol, Condensed Tannin and Flavonoid Contents and Antioxidant Activity of *Uncaria gambir* Extracts. *Indonesian Journal of Pharmacy*, **22**(1); 50–59

Kushwaha, S. K., R. K. Keshari, and A. Rai (2011). Advances in Nasal Trans-Mucosal Drug Delivery. *Journal of Applied Pharmaceutical Science*, **1**(7); 21–28

Lee, D. and T. Minko (2021). Nanotherapeutics for Nose-To-Brain Drug Delivery: An Approach to Bypass the Blood Brain Barrier. *Pharmaceutics*, **13**(2); 2049

Mardiyanto, M., H. Herlina, N. A. Fithri, and Y. Rahmi (2019). Formulasi Dan Evaluasi Sediaan Submikro Partikel Gelasi-Ionik Pembawa Ekstrak Daun *Pluchea Indica* Sebagai Antibakteri Pada Kulit Tikus Putih Jantan Galur Wistar. *Jurnal Sains Farmasi & Klinis*, **6**(2); 171–179 (In Indonesia)

Melia, S., D. Novia, and I. Juliyarsi (2015). Antioxidant and Antimicrobial Activities of Gambir (*Uncaria gambir* Roxb.) Extracts and Their Application in Rendang. *Pakistan Journal of Nutrition*, **14**(12); 938

Molyneux, P. (2004). The Use of the Stable Free Radical Diphenylpicrylhydrazyl (DPPH) for Estimating Antioxidant Activity. *Songklanakarin J. sci. technol*, **26**(2); 211–219

Nazir, N. (2000). *Gambir: Budidaya, Pengolahan, Dan Prospek Diversifikasinya*. Yayasan Hutanku, Bogor, Indonesia (In Indonesia)

Pambayun, R., M. Gardjito, S. Sudarmadji, and K. Kuswanto (2007). Catechin Type Extracted from Gambier Commercial Which Has the Strongest Antibacterial Activity. *Jurnal Agribisnis dan Industri Pertanian*, **6**(1); 49–55

Pardeshi, C. V. and V. S. Belgamwar (2013). Direct Nose to Brain Drug Delivery Via Integrated Nerve Pathways Bypassing the Blood-Brain Barrier: An Excellent Platform for Brain Targeting. *Expert Opinion on Drug Delivery*, **10**(7); 957–972

Pawar, N. and H. Chaudhary (2015). Non-Pressurized Topical Spray of Diclofenac Diethylamine. *International Journal Advances in Pharmaceutics*, **4**(4); 40–8

Peng, Y., H. Jin, Y.-h. Xue, Q. Chen, S.-y. Yao, M.-q. Du, and S. Liu (2023). Current and Future Therapeutic Strategies for Alzheimer's Disease: An Overview of Drug Development Bottlenecks. *Frontiers in Aging Neuroscience*, **15**; 1–16

Pervin, M., M. A. Hasnat, Y. M. Lee, D. H. Kim, J. E. Jo, and B. O. Lim (2014). Antioxidant Activity and Acetylcholinesterase Inhibition of Grape Skin Anthocyanin (GSA). *Molecules*, **19**(7); 9403–9418

Pohanka, M., M. Hrabinova, K. Kuca, and J.-P. Simonato (2011). Assessment of Acetylcholinesterase Activity Using Indoxylacetate and Comparison with the Standard Ellman's Method. *International Journal of Molecular Sciences*, **12**(4); 2631–2640

Rajaram, S. and R. Natham (2013). Influence of Formulation and Process Variables on the Formation of Rifampicin Nanoparticles by Ionic Gelation Technique. *RJPBCS*, **4**; 820–832

Ramvikas, M., M. Arumugam, S. Chakrabarti, and K. Jaganathan (2017). Nasal Vaccine Delivery. In *Micro and Nanotechnology in Vaccine Development*. Elsevier, pages 279–301

Ranjan, N. and M. Kumari (2016). Inhibitory Activity of Acetylcholinesterase (AChE) and Antioxidant Activity of Methanolic Extract of *Desmodium angeticum* (L.). *International Journal of Bioassays*, **6**(1); 5208–5210

Ribeiro, E. F., T. T. de Barros-Alexandrino, O. B. G. Assis, A. C. Junior, A. Quiles, I. Hernando, and V. R. Nicoletti (2020). Chitosan and Crosslinked Chitosan Nanoparticles: Synthesis, Characterization and Their Role As Pickering Emulsifiers. *Carbohydrate Polymers*, **250**; 116878

Sachdeva, B., P. Sachdeva, A. Negi, S. Ghosh, S. Han, S. Dewanjee, S. K. Jha, R. Bhaskar, J. K. Sinha, A. C. Paiva-Santos (2023). Chitosan Nanoparticles-Based Cancer Drug Delivery: Application and Challenges. *Marine Drugs*, **21**(4); 211

Salatin, S., J. Barar, M. Barzegar-Jalali, K. Adibkia, F. Kiafar, and M. Jelvehgari (2017). Development of a Nanoprecipitation Method for the Entrapment of a Very Water Soluble Drug into Eudragit RL Nanoparticles. *Research in Pharmaceutical Sciences*, **12**(1); 1–14

Sazwi, N. N., T. Nalina, and Z. H. A. Rahim (2013). Antioxidant and Cytoprotective Activities of *Piper betle*, *Areca catechu*, *Uncaria gambir* and Betel quid with and without Calcium Hydroxide. *BMC Complementary and Alternative Medicine*, **13**; 1–12

Sinko, P. J. (2023). *Martin's Physical Pharmacy and Pharmaceutical Sciences*. The State University of New Jersey

Sukweenadhi, J., F. Setiawan, O. Yunita, K. Kartini, and C. Avanti (2020). Antioxidant Activity Screening of Seven Indonesian Herbal Extract. *Biodiversitas*, **21**(5); 2062–2067

Taléns-Visconti, R., J. V. de Julián-Ortiz, O. Vila-Busó, O. Diez-Sales, and A. Nácher (2023). Intranasal Drug Administration in Alzheimer-Type Dementia: Towards Clinical Applications. *Pharmaceutics*, **15**(5); 1399

Ünver, Y., S. Deniz, F. Çelik, Z. Akar, M. Küçük, and K. Sancak (2016). Synthesis of New 1, 2, 4-Triazole Compounds Containing Schiff and Mannich Bases (Morpholine) with Antioxidant and Antimicrobial Activities. *Journal of Enzyme Inhibition and Medicinal Chemistry*, **31**(3); 89–95

van der Flier, W. M., M. E. de Vugt, E. M. Smets, M. Blom, and C. E. Teunissen (2023). Towards a Future Where Alzheimer's Disease Pathology Is Stopped before the Onset of Dementia. *Nature Aging*, **3**(5); 494–505

van Woensel, M., N. Wauthoz, R. Rosière, K. Amighi, V. Mathieu, F. Lefranc, S. W. Van Gool, and S. De Vleeschouwer

(2013). Formulations for Intranasal Delivery of Pharmacological Agents to Combat Brain Disease: A New Opportunity to Tackle Gbm? *Cancers*, **5**(3); 1020–1048

Wu, D., Q. Chen, X. Chen, F. Han, Z. Chen, and Y. Wang (2023a). The Blood-Brain Barrier: Structure, Regulation, and Drug Delivery. *Signal Transduction and Targeted Therapy*, **8**(1); 217

Wu, M.-Y., I.-F. Kao, C.-Y. Fu, and S.-K. Yen (2023b). Effects of Adding Chitosan on Drug Entrapment Efficiency and Release Duration for Paclitaxel-Loaded Hydroxyapatite-Gelatin Composite Microspheres. *Pharmaceutics*, **15**(8); 2025

Yeni, G., K. Syamsu, O. Suparno, E. Mardliyati, and H. Muchtar (2014). Repeated Extraction Process of Raw Gambiers (*Uncaria gambir* Robx.) for the Catechin Production As an Antioxidant. *International Journal of Applied Engineering Research*, **9**(24); 24565–24578

Yunarto, N. and N. Aini (2015). Effect of Purified Gambir Leaves Extract to Prevent Atherosclerosis in Rats. *Health Science Journal of Indonesia*, **6**(2); 105–110

